Title
Methods for fatigue testing off-road bicycle handlebars based on assembly effects using two different stem designs

Journal
Journal of Testing and Evaluation, 31(2)

ISSN
0090-3973

Authors
McKenna, Sean P
Hill, Michael R
Hull, Maury L

Publication Date
2003-03-01

Peer reviewed

Journal of Testing and Evaluation, Vol. 31, No. 2
Paper ID JTE10903_312
Available online at: www.astm.org

Sean P. McKenna,[1] *Michael R. Hill,*[1] *and Maury L. Hull*[1]

Methods for Fatigue Testing Off-Road Bicycle Handlebars Based on Assembly Effects Using Two Different Stem Designs

ABSTRACT: Assembly of off-road bicycle handlebars with a stem that clamps the handlebar around its circumference would be expected to affect fatigue performance by introducing both assembly stresses and stress concentration. Because the effect of clamping on fatigue performance is unknown and because of the need to insure structural reliability in the stem-handlebar assembly to prevent serious injury, the objectives of the work reported by the present article were fourfold. One was to determine the stresses due to assembly and the stress concentration induced in a handlebar for two different clamp designs (i.e. 1-bolt and 2-bolt), a second was to determine experimentally the high cycle constant amplitude load fatigue lives of the two stem-handlebar assemblies, a third was to determine experimentally the variable amplitude load fatigue lives, and the fourth was to predict the variable amplitude load fatigue life with constant amplitude load fatigue test results. The handlebar was instrumented with strain gages and the assembly strains were measured when the stem clamps were tightened. The handlebar was also loaded as a cantilever beam while the applied strains were measured for each assembly. Stresses were computed and the maximum stresses induced by clamping exceeded 200 MPa for both assemblies. A method unique to this study was devised to determine the stress concentration at an arbitrary angular location around the circumference of the handlebar and for an arbitrary loading direction in the plane of the bicycle. For a load directed along an angle of −38° (clockwise rotation from horizontal viewed from the right), both stems created similar stress concentration; the location of maximum applied stress was shifted by 30° from the point that would be expected in the absence of assembly and the stress was increased by 40% at this location. The measured fatigue lifetimes for constant amplitude loading were similar for the two stem designs but the variable amplitude load fatigue lifetime for the 1-bolt stem assembly was shorter than that for the 2-bolt stem assembly by 19%. The fatigue lifetimes for variable amplitude loading based on constant amplitude load fatigue test results were predicted to within 3% and 33% for the 1-bolt and 2-bolt stems, respectively. Thus, constant amplitude load fatigue test results can be used to approximate the variable amplitude load fatigue life. However, the ranking of different assemblies may not be accurately indicated by constant amplitude load fatigue data.

KEYWORDS: bicycle, handlebar, fatigue, assembly, stress concentration

Failure of bicycle components such as the handlebar can result in a loss of steering and braking control and/or a lack of support for the rider's weight, thereby leading to serious injury [1,2]. Unfortunately, assuring structural integrity of such components in both the design and product qualification stages is complicated by difficulties arising from the connections inherent in these assemblies. For example, assembly of components by either press fit (e.g., crank arm on bottom bracket spindle) or clamp (e.g., handlebar in stem) introduces stress as a result of the clamping process and also creates a stress concentration as a result of abrupt change in stiffness. These assembly effects are difficult to quantify using theoretical models, thus complicating the design process, particularly in analytically predicting high cycle fatigue failure.

Moreover, because bicycle manufacturers mix and match components from different suppliers, one particular assembly may be formed from components with a variety of structural differences. The degree to which these differences affect the ability of the assembly to withstand the loads placed on it by the environment is unknown. If it could be determined whether the structural differences in components affect the high cycle fatigue life, then this knowledge would be useful in both product design and qualification. The broad goal of the work reported in this article was to determine whether the structural differences in two stem-handlebar assemblies give rise to differences in the high cycle fatigue life of these assemblies.

There are a variety of bicycle stems on the market, and each stem's clamp design will impart unique assembly stresses onto the handlebar and give rise to a unique stress concentration. The two basic stem-clamping designs are the 1-bolt and 2-bolt designs (Fig. 1). The 2-bolt design has a clamp with two parts attached by two bolts, one above the horizontal handlebar axis and one below. For the 1-bolt design, part of the stem clamp wraps around the handlebar and bolts together with a single bolt on the underside of the stem. Due to the different nature of the clamps, each stem will likely impart different assembly stresses into the handlebar and cause a different stress concentration. Thus, the first objective was to determine assembly stress and stress concentration for two different stem designs on one handlebar and to assess the effects of assembly.

If these two stem designs impart different assembly effects to the handlebar, then these effects may cause differences in the fatigue lifetime of the handlebar. To detect these differences, it is important that stem-handlebar assemblies be fatigue tested under realistic conditions in the presence of all influencing factors. To consider all factors such as clamp edge geometry, fretting, and assembly effects, the handlebar must be fatigue tested with the stem attached. Thus the second objective was to determine experimentally the high cycle fatigue life of the handlebar for two different

Manuscript received 11/5/2001; accepted for publication 10/15/2002; published XXXX.

[1] Research Assistant, Assistant Professor, and Professor, respectively, Department of Mechanical and Aeronautical Engineering, University of California, One Shields Avenue, Davis, CA 95616.

stem-handlebar assemblies under constant amplitude loading. A related objective was to use the information gleaned from the first objective above to interpret results from the constant amplitude loading tests for the two assemblies.

Because of the simplicity of constant amplitude load testing in conjunction with the need to insure a safe product, constant amplitude load testing is the preferred method for qualifying products for fatigue performance in the bicycle industry. Currently, the ISO Standard 4210 [3] for qualifying stem-handlebar assemblies calls for constant amplitude load testing. The development and widespread adoption of such a standard helps ensure that all companies test bicycle components in the same way, and therefore provide safer bicycles across the industry. However, constant amplitude load testing may not provide an accurate assessment of failure propensity because the bicycle field loading is not constant amplitude [4,5]. Studies on riveted lap joint assemblies of different materials have shown that the best performing assembly under constant amplitude loading was the worst performing assembly under variable amplitude loading [6]. To fully understand the in-service fatigue performance of the stem-handlebar assembly, testing this assembly under variable amplitude loading is imperative. As in the constant amplitude load case, effects from factors related to clamping will influence fatigue failure in ways that can be determined only through testing. Thus, the third objective was to determine experimentally the variable amplitude load high cycle fatigue lifetimes for the two different stem-handlebar assemblies.

While variable amplitude loading must be considered in order to gain a more realistic picture of the fatigue performance under field loading of the stem-handlebar assembly, variable amplitude load analysis and testing add complications to the study of high cycle fatigue. However, if it can be determined that the fatigue behavior of stem-handlebar assemblies is indicated well by constant amplitude load testing, then this would simplify both design and testing. Thus, a fourth objective was to predict the variable amplitude load fatigue life from the constant amplitude load test results and determine whether such a simplification is possible by comparing the predicted life with that from the variable amplitude load test results.

Methods

Materials

Two stems and one handlebar were chosen from typical commonly available components for off-road bicycles. One stem was a 1-bolt stem, where the clamshell-style handlebar clamp bolted together on the underside of the stem (Fig. 1). The 1-bolt stem was made of steel and had no riser angle, meaning that the stem extension was perpendicular to the quill. The other stem was a 2-bolt stem, which had a front plate that used two bolts to clamp the handlebar in place (Fig. 1). The 2-bolt stem was made of aluminum and had a 10° rise angle. The 1-bolt stem measured 35 mm across the clamp and the 2-bolt stem measured 50 mm across the clamp. The edge of the clamps at the clamp-handlebar junction differed in that the edge of the 1-bolt stem was a corner, while the edge of the 2-bolt stem was rounded (radius approximately 1 mm). The handlebar was 580 mm long and had a nominal outside diameter of 25.4 mm and an inside diameter of 21.0 mm. The bar was made of 6061-T6 aluminum (Table 1) and was bent at 6° (Fig. 2).

Quantifying Assembly Effects

An instrumented handlebar and a bolt force transducer were constructed to determine the assembly stress around the outer surface of the handlebar. To measure strains in the handlebar, four perpendicular strain gage rosettes were mounted on a circumference on the outer surface of the handlebar at 90° intervals so that the gages were oriented in the longitudinal and transverse directions of the handlebar. The longitudinal direction was along the length of the handlebar.

To ensure consistency in the clamping force when tightening the stem clamp bolt(s), the bolt force (i.e., tension) was measured. Bolt force was measured rather than tightening torque because tighten-

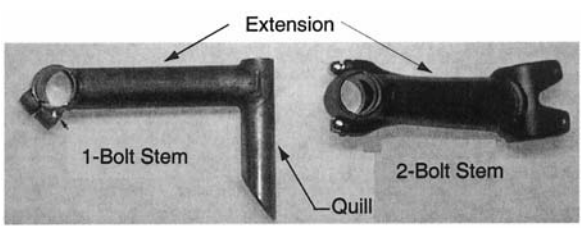

FIG. 1—*Photograph of the 1-bolt and 2-bolt stems used in this study.*

TABLE 1—*Handlebar geometry and material properties for 6061-T6 aluminum [10].*

Modulus of elasticity	73.1 GPa
Ultimate strength	310 MPa
Yield strength	276 MPa
Poisson's ratio	0.345
Walker equation exponent	0.63
Outer diameter of middle section	25.4 mm
Inner diameter of middle section	21.0 mm

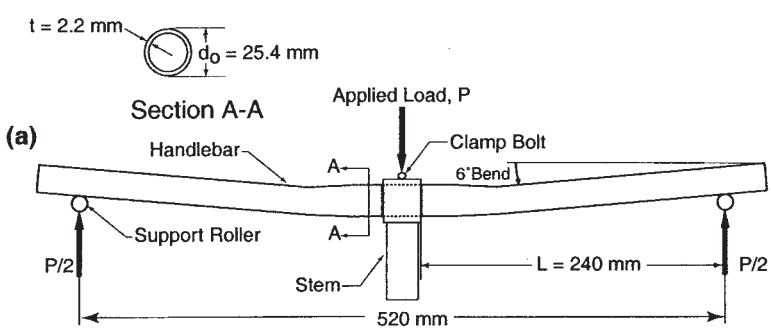

FIG. 2—*Diagram of a handlebar in 3-point bending.*

ing torque does not consistently indicate bolt force as a consequence of friction between the threads [7,8]. A bolt force transducer was made by mounting strain gages onto a steel sleeve that was sandwiched between the stem and the head of the bolt. The stem clamp bolt(s) were tightened until a strain corresponding to a tightening torque of 11.4 Nm (100 in.-lb) was indicated by the bolt force transducer. For the 2-bolt stem, a feeler gage was used to ensure the same clamp gap at each bolt.

The assembly strain around the circumference of the handlebar was measured at 10° intervals by repeatedly tightening the stem clamp bolt(s) for different rotations of the instrumented handlebar relative to the stem. During these measurements, the center of the strain gages was positioned 1.6 mm away from the edge of the stem clamp. Longitudinal ($\sigma_{L,ass}$) and transverse ($\sigma_{T,ass}$) assembly stresses were computed from the strains measured at different points around the circumference of the handlebar after the stem clamp bolts were tightened. Stresses were computed by assuming elastic deformation in plane stress:

$$\sigma_{L,ass} = \frac{E(\varepsilon_L + v\varepsilon_T)}{1 - v^2} \quad (1)$$

$$\sigma_{T,ass} = \frac{E(\varepsilon_T + v\varepsilon_L)}{1 - v^2} \quad (2)$$

where E is the modulus of elasticity (Table 1), ν is Poisson's ratio, ε_T is the measured transverse strain, and ε_L is the measured longitudinal strain.

The clamped handlebar was loaded in two orthogonal directions to map the stress due to bending around the outer circumference of the handlebar next to the edge of the stem clamp. Loading in orthogonal directions was required because there is minimal stress along the neutral axis from cantilever bending. Three load values were applied near the end of the handlebar at each of two directions separated by 90°. The two loading directions were $\theta_b = 197°$ and $\theta_b = 287°$, which were perpendicular to and along the steering axis, respectively (Fig. 3). Strains were recorded in the longitudinal and transverse directions for each load with the handlebar rotated in 10° increments and with the gages positioned 1.6 mm away from the edge of the stem clamp.

Stress concentration was quantified using normalized bending stress. Because the stress concentration factor is undefined on the neutral axis, it was not a useful quantity in present study. The normalized bending stress σ_N was defined as the ratio of the longitudinal stress $\sigma_{L,b}$ to the maximum bending stress computed from beam theory in the absence of any stress concentration and was determined from

$$\sigma_N(\alpha,\theta_b) = \left(\frac{I}{WLr_o}\right)\sigma_{L,b}(\alpha,\theta_b,W,L) \quad (3)$$

where W is the weight applied to the end of the bar for a given value of $\sigma_{L,b}$, L is the distance from the point of load application to the edge of the stem, I is the moment of inertia of the handlebar cross section, and r_o is the outer radius of the handlebar. The equation acknowledges the dependence of σ_N on the angle of loading α and on the angular position around the stem θ_b.

To determine the normalized bending stress within the context of the definition above, strains were measured due to the cantilevered loads, and the longitudinal stress $\sigma_{L,b}$ was calculated from an equation analogous to Eq 1. The normalized bending stress was determined for each of the three loads in the experiment, and these values were averaged at a given point to reduce uncertainty.

Because the normalized bending stress at the same point θ_b differs for the two orthogonal loading directions, two contributions to the normalized bending stress exist, one corresponding to loads applied in the X-direction (B_X) and the other to loads applied in the Z-direction (B_Z). The respective contributions are given by

$$B_X(\theta_b) = \sin(287°)\sigma_N(197°,\theta_b) - \sin(197°)\sigma_N(287°,\theta_b) \quad (4)$$

$$B_Z(\theta_b) = -\cos(287°)\sigma_N(197°,\theta_b) + \cos(197°)\sigma_N(287°,\theta_b) \quad (5)$$

To appreciate the stress concentration induced by the stem-handlebar assemblies, the normalized bending stress contributions at each point around the handlebar circumference were computed and were compared to the bending stress at each point due to beam theory (i.e., no stress concentration). If no stress concentration was present, then B_X would be equal to a negative cosine function with unit amplitude and B_Z would be equal to a negative sine function with unit amplitude. The discrepancies between the actual normalized bending stress contributions and their corresponding theoretical trigonometric functions are an effect of the assembly of the stem-handlebar.

Constant Amplitude Load Fatigue Testing

Fatigue testing of the stem-handlebar assembly was conducted in 3-point bending (Fig. 2, Fig. 4). The actuator was connected to

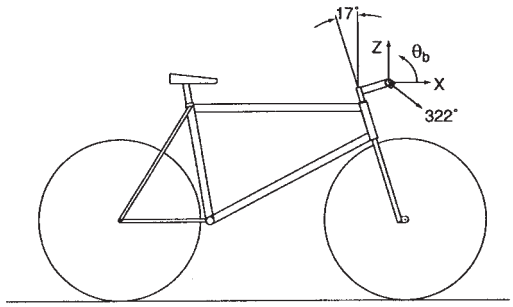

FIG. 3—*Diagram illustrating the reference frame used for the bicycle.*

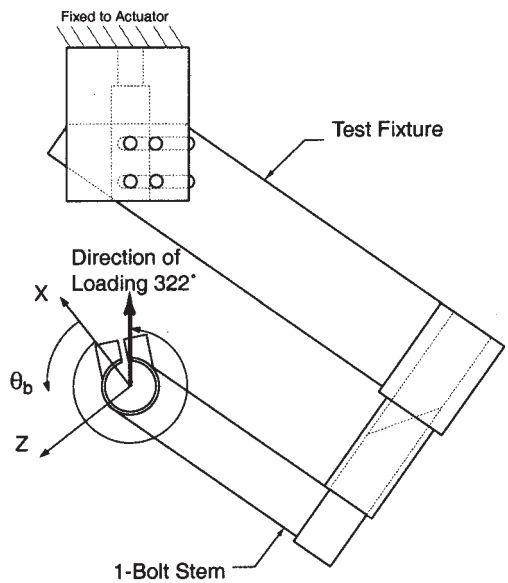

FIG. 4—*Diagram of fatigue test fixture designed to load both stems at the direction of maximum damage 322°.*

the part of the fixture that held the stem. The handlebar rested on two rollers supported by an arm that spanned the length of the handlebar that was in turn attached to the load cell. This fixture loaded the handlebar at an angle $\alpha = 322°$.

To map the load-life curve for the assembly, five load ranges (maximum load = 1.20, 1.40, 1.70, 1.89, and 2.10 kN) were used at $R = 0.1$ to obtain lifetimes between 10^4 and 10^6 cycles. Five samples were tested at each load range, thus requiring a total of 25 constant amplitude load experiments for each stem-handlebar assembly. Fatigue tests were terminated when the compliance (as indicated by the displacement of the actuator) increased 10% compared to the compliance at the beginning of the test. After each fatigue test, the location of crack initiation was determined by observing the fracture surface under magnification and noting where the crack growth started. Using intervals of 5°, a histogram of the locations of crack initiation was constructed to illustrate the most common failure locations.

Interpretation of Fatigue Lifetimes

To interpret the constant amplitude load fatigue performance for the two assemblies, the stresses induced in the handlebar were of interest. The stress history at a given point around the handlebar circumference near the edge of the stem can be found from the measured normalized bending stress and the measured assembly stress. The bending stress $\sigma_{app}(\theta_b, t)$ around the handlebar circumference due to externally applied loads to the handlebar can be determined by multiplying the maximum bending stress for a time series of force components applied along the *X*- and *Z*-directions by the corresponding normalized bending stress contributions:

$$\sigma_{app}(\theta_b,t) = \frac{Lr_o}{I}\left[B_x(\theta_b)F_x(t) + B_z(\theta_b)F_z(t)\right] \tag{6}$$

where $F_X(t)$ and $F_Z(t)$ are the force components applied near the end of the handlebar along the *X*- and *Z*-directions, respectively. Unlike the applied bending stress, the assembly stress does not vary with time and therefore can be treated as an effective mean stress. Sines's method [9] was used to account for the effect of the biaxial assembly stress in fatigue. Sines's method suggests that an effective mean stress $\sigma_{m,ass}$ is the sum of the assembly stress components in the longitudinal and transverse directions

$$\sigma_{m,ass}(\theta_b) = \sigma_{L,ass}(\theta_b) + \sigma_{T,ass}(\theta_b) \tag{7}$$

The total stress σ_{Tot}, which is active in fatigue, can then be determined as the sum of the applied and effective mean stresses as a function of the angle σ_b around the handlebar circumference from

$$\sigma_{Tot}(t,\theta_b) = \sigma_{app}(t,\theta_b) + \sigma_{m,ass}(\theta_b) \tag{8}$$

Inasmuch as the total stress was a function of time in the fatigue tests, the Walker equivalent stress was determined because this quantity could account for both the applied stress created by the load cycle and the effective mean stress created by the assembly. To compute the equivalent stress, the maximum and minimum applied stresses around the handlebar for the specific angle of loading ($\alpha = 322°$) used in the tests were computed using Equation 6 with $F_X = P\cos(\alpha)/2$ and $F_Z = P\sin(\alpha)/2$ where *P* was the maximum and minimum magnitudes of the test load applied to the stem. These stresses were then substituted into Eq 8 to determine the maximum $\sigma_{Tot,max}$ and minimum $\sigma_{Tot,\,min}$ total stresses at 1° increments around the handlebar. The Walker equivalent stress σ_{eq} was computed from

$$R(\theta_b) = \frac{\sigma_{Tot,min}(\theta_b)}{\sigma_{Tot,max}(\theta_b)} \tag{9}$$

$$\sigma_{eq}(\theta_b) = \sigma_{Tot,max}(\theta_b)(1 - R(\theta_b))^{0.63} \tag{10}$$

where *R* is the stress ratio and the Walker equation exponent 0.63 was reported with reference data for 6061-T6 aluminum [10]. The angular location of the largest equivalent stress is the predicted location of failure, which was compared to the histogram of failure locations from the fatigue tests.

Variable Amplitude Load Testing

The loads used in the variable amplitude load fatigue tests were determined from a database of handlebar force data measured while riding downhill on an instrumented full-suspension mountain bike [4]. During a 30 s ride, force components applied by the rider to the handlebar in both the *X*- and *Z*-directions (Fig. 3) were recorded every 5 ms on both sides of the handlebar. Seven different riders each rode twice in the standing position with the rear suspension active for one ride and inactive for the other ride. Each side of the handlebar was considered independently. Therefore, a total of 28 different 30 s ride trials was available from these earlier tests.

To determine a program of loading of reasonable duration to represent the variable amplitude loading, the load data were filtered using a sequence of steps. First, the bending stress histories were computed at $\theta_b = 142°$ (opposite the direction of loading used in the test, 322°), discounting assembly effects. Assembly effects were discounted in determining the test loads because the loading was to be independent of any particular stem. The resulting bending stress histories from all of the 28 trials were combined and rainflow counted as one long trial. Next, rainflow counted cycles with amplitude and mean stress pairs were used to calculate an equivalent stress cycle that could be used with the test fixture. This was a necessary step for cycles with minimum stress less than zero because the fixture was designed to be loaded only in compression. The equivalent stress cycle was found using the Walker equation (Eqs 9 and 10) and a minimum stress corresponding to a minimum load of 50 N. This produced a stress cycle that theoretically induced the same damage as the original amplitude and mean stress pair from rainflow counting. Next, the cycles that were small and caused minute damage (i.e., σ_{eq} less than 50% of the fatigue strength at 10^8 cycles) were omitted [11]. To further accelerate the fatigue testing, the low stress filter level was raised to 82% of the fatigue strength at 10^8 cycles. The 82% screening level removed only 0.1% of the total damage but decreased the testing time by a factor of two. As a consequence of loading in compression, the test fixture inhibited testing at the two highest stresses. They were omitted for two reasons. One reason was because the maximum stress computed from the Walker equation exceeded the ultimate strength of the handlebar. The other reason was that the two highest omitted stresses never occurred in any of the 28 trials when each trial was rainflow counted individually.

Finally, a maximum load P_{max} was determined for each of the filtered stress cycles and the maximum loads for all cycles were grouped into blocks. The maximum stress σ_{max} foreach of the filtered stress cycles was converted into a corresponding maximum load using.

$$P_{max} = \frac{2I\sigma_{max}}{L_t r_o} \tag{11}$$

where L_t = 26 cm (half the distance between the two support rollers). The filtered loads were then grouped by magnitude within ±5% into the same block. The maximum load of each of the counted reversals within a block was used for the maximum test load for that block. The blocks then were ordered sequentially in order of descending maximum load. The variable amplitude load fatigue testing was conducted in an identical manner as the constant amplitude load fatigue testing except that the sequence of blocks was repeated until the stem-handlebar assembly failed by the compliance criterion.

Variable Amplitude Load Fatigue Life Prediction

The variable amplitude load fatigue life for each stem was predicted based on data from the constant amplitude load fatigue testing. As a first step, the Walker equivalent load was related to the lifetime data from the constant amplitude load fatigue tests. Using least squares analysis, a power function was curve fit to the constant amplitude load lifetime data to obtain an empirical relationship between maximum applied force and fatigue lifetime. The form of the power function was:

$$P_{max} = A(N_f)^b \tag{12}$$

where N_f is the number of cycles to failure, A is the power function factor, and b is the power function exponent. However, the constant amplitude load fatigue tests were for R = 0.1 and the variable amplitude loads had R-values ranging from 0.027 to 0.053 because the minimum load was 50 N for all blocks. To account for the different R-values, each load ratio in the constant amplitude loading was placed in Eq 10 with P_{eq} substituted for σ_{eq} to determine a Walker equivalent load P_{eq}. The power law relating the Walker equivalent load to the number of cycles to failure became

$$P_{eq} = A^*(N_f)^{b^*} \tag{13}$$

where $A^* = A(1\text{-}R)^{0.63}$ and $b^* = b$.

To predict the fatigue life under variable amplitude loading, the Walker equivalent load $P_{eq,i}$ was determined for each block of load (denoted by i) in the variable amplitude loading sequence and the corresponding damage was determined. The equivalent load for each block was computed from Eqs 9 and 10 with P_{max} for the block and P_{min} = 50 N replacing the corresponding values of σ. Equation 13 was rearranged and solved for the expected number of cycles to failure $N_{f,i}$ for a given Walker equivalent load $P_{eq,i}$

$$N_{f,i} = \left(\frac{P_{eq,i}}{A^*}\right)^{1/b^*} \tag{14}$$

With each block of load consisting of a number of cycles n_i, the damage D_i associated with a given block of equivalent load $P_{eq,i}$ was computed using Miner's linear damage rule [12,13]:

$$D_i = \frac{n_i}{N_{f,i}} \tag{15}$$

Summing the damage for all of the blocks, the variable amplitude load fatigue lifetime was estimated in terms of the number of load sequences to failure N_s from

$$N_s = \frac{1}{\sum_{i=1}^{m} D_i} \tag{16}$$

where m is the number of blocks within the load sequence.

Results

Attachment of both stems introduced substantial assembly stresses into the handlebar for both the 1-bolt and 2-bolt stems and the effects of assembly were comparable for some quantities notwithstanding the differences in the clamp designs (Fig. 5). For the 1-bolt stem, the longitudinal assembly stress was generally positive with local peaks of 92.5 MPa and 104.3 MPa occurring at θ_b = 147° and 327°, respectively. Similarly the 2-bolt stem had local peaks of 107 MPa and 111 MPa occurring at θ_b = 122° and 302°, respectively. The minimum longitudinal stresses of −2.8 MPa and −15.3 MPa introduced by the 1-bolt stem were relatively small in magnitude and occurred at θ_b = 47° and 207°, respectively. In contrast the 2-bolt stem had minimum longitudinal stresses of −77 MPa and −104 MPa, which were much larger in magnitude than those for the 1-bolt stem, yet they occurred at similar angles of θ_b = 32° and 212°, respectively.

The maximum transverse assembly stress of 116.7 MPa occurring at θ_b = 287° for the 1-bolt stem and the maximum transverse stress of 112 MPa occurring at θ_b = 302° for the 2-bolt stem were comparable in both magnitude and location. However, the minimum transverse stress of −197.1 MPa occurring at θ_b = 197° for the 1-bolt stem and the minimum transverse stress of −246 MPa occurring at θ_b = 212° for the 2-bolt stem were different in magnitude but comparable in location.

In examining the normalized bending stress contributions around the handlebar for the two orthogonal load directions (Fig. 6, Table 2), the effects of the stress concentration were similar between the two stems. For the 1-bolt stem the largest value of B_X was 1.41 at θ_b = 187° and the largest value of B_Z was 1.32 at θ_b = 247°. Similarly the 2-bolt stem had a maximum B_X of 1.45 at θ_b = 182° and the largest value of B_Z was 1.27 at θ_b = 252°.

The constant amplitude load fatigue test results showed that the lifetimes for both stem-handlebar assemblies were similar (Fig. 7), but that the sites of crack initiation were different. For the 1-bolt stem, most cracks initiated at 170° (Fig. 8). For the 2-bolt stem however, most cracks initiated at 150° (Fig. 9).

The equivalent stresses were consistent with the findings from the constant amplitude load fatigue tests. The maximum equivalent

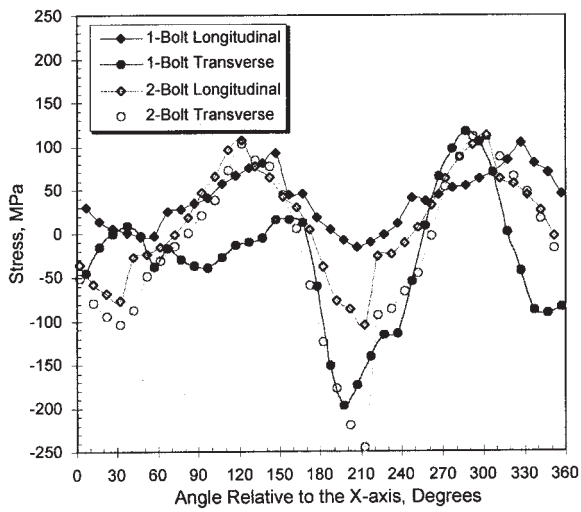

FIG. 5—*Plot of longitudinal and transverse stresses from the stem-handlebar assembly as a function of the angle relative to the X-axis. Results are for the 1-bolt and 2-bolt stem-handlebar assemblies clamped with a force equivalent to a clamping torque of 11.4 Nm.*

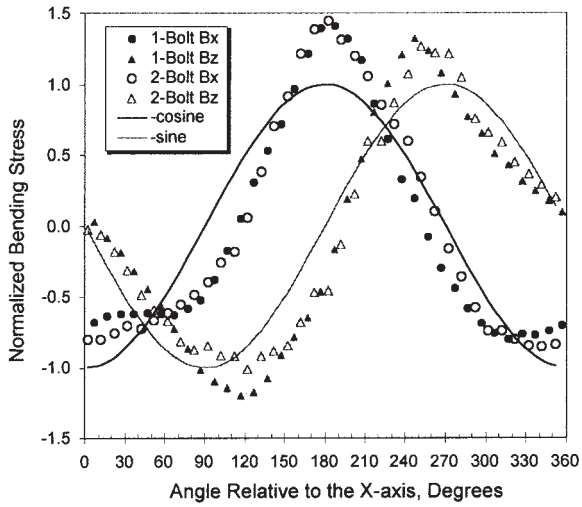

FIG. 6—*Plot of stress concentration contributions from loading in the X and Z-directions with the 1-bolt and 2-bolt stems and normalized theoretical bending stress from beam theory as a function of angle relative to the X-axis.*

TABLE 2—*Maximum values of assembly effects and their positions relative to the X-axis for the 1 and 2–bolt stems.*

	1-Bolt Stem		2-Bolt Stem	
	Magnitude	Angle	Magnitude	Angle
Maximum $\sigma_{T,ass}$	116 MPa	287°	112 MPa	302°
Maximum $\sigma_{L,ass}$	104 MPa	327°	111 MPa	302°
Maximum $\sigma_{m,ass}$	172 MPa	287°	223 MPa	302°
Maximum B_X	1.41	187°	1.45	182°
Maximum B_Z	1.32	247°	1.27	252°
Maximum σ_{Tot}, α = 322°, 1700 N applied load	387 MPa	167°	399 MPa	162°
Maximum σ_{eq}, α = 322°, 1700 N applied load	327 MPa	167°	315 MPa	162°

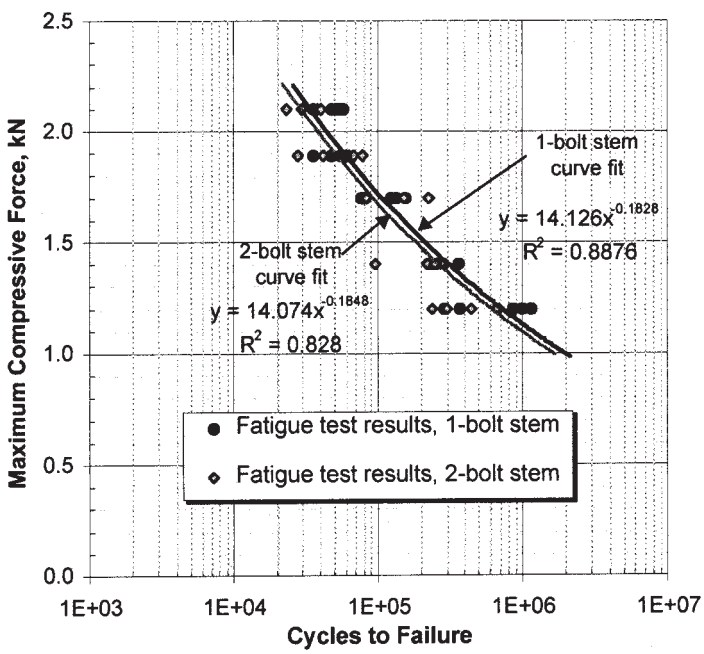

FIG. 7—*Plot comparing experimental constant amplitude load fatigue lives for both stem-handlebar assemblies and power law curve fits.*

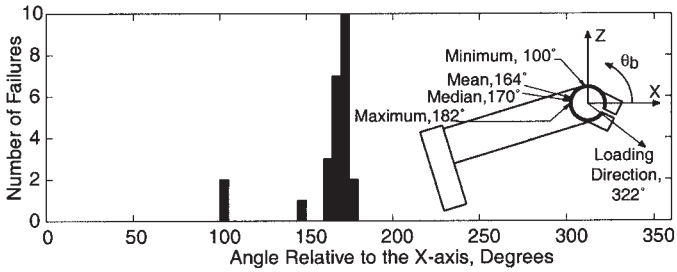

FIG. 8—*Histogram of experimental locations of fatigue crack initiation in the constant amplitude load tests relative to the X-axis for the 1-bolt stem.*

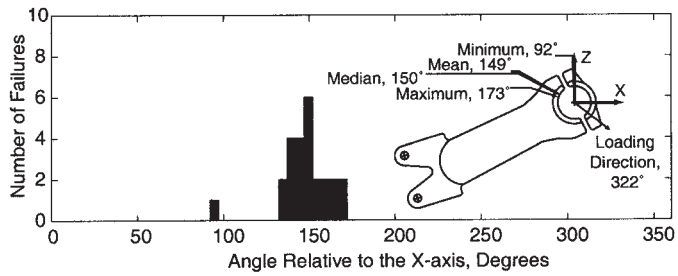

FIG. 9—*Histogram of experimental locations of fatigue crack initiation for the constant amplitude load tests relative to the X-axis for the 2-bolt stem.*

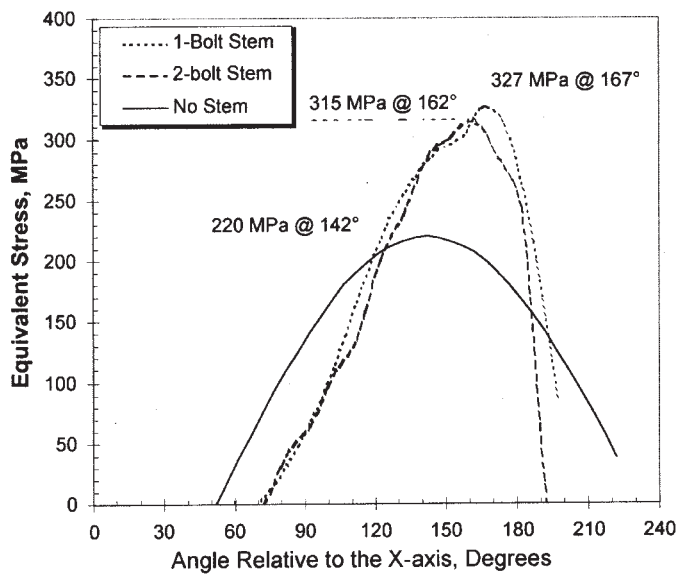

FIG. 10—*Plot of equivalent stress in the handlebar as a function of angle relative to the X-axis for the 1-bolt and 2-bolt stems and no stem. Stresses are calculated for load P = 1.7 kN and R = 0.1.*

stresses for a 1700 N applied load were similar both in magnitude (327 and 315 MPa for 1-bolt and 2-bolt stems, respectively) and in angular location (167° and 162° for 1-bolt and 2-bolt stems, respectively) (Fig. 10, Table 2). The similarity occurred because both the assembly stresses in the longitudinal direction (Fig. 5) and the stress concentration in the two orthogonal load directions (Fig. 6) were also similar for the two stem-handlebar assemblies. The angular locations of maximum equivalent stress (i.e., predicted locations of failure) for the 1-bolt and 2-bolt stems differed by only 3° and 12°, respectively, from the most common failure locations determined experimentally.

Block loading for the variable amplitude load testing was conducted with five distinct load ranges (Table 3). Each range had a minimum load of 50 N and the five maximum loads were 1840, 1596, 1523, 1402, and 949 N with each range repeated 1, 1, 8, 8, and 221 times, respectively, within a sequence and the sequence repeated until failure.

The variable amplitude load fatigue life for the 1-bolt stem was shorter than that for the 2-bolt stem. The average life was 4806 sequences for the 1-bolt stem, which was 19% shorter than that for the 2-bolt stem that had a life of 5920 sequences (Table 4). For the 1-bolt stem, most cracks initiated at 169°, which was only 2° different from the location in the constant amplitude load tests. For the 2-bolt stem, most cracks initiated at 156°, which was only 6° away from the most common location in the constant amplitude load tests.

The life predictions based on the constant amplitude load fatigue data adjusted for load ratio predicted the variable amplitude load fatigue test life well for one stem-handlebar assembly but not as well for the other. The predicted life for the 1-bolt stem was 4674 sequences (Table 3), which was less than the average value of the measured life by 3%. The predicted life for the 2-bolt stem was 3973 sequences, which was less than the average value of the measured life by 33%.

Discussion

Because structural failure of the handlebar in the off-road environment could lead to serious injury and because a variety of stems are used that impart different assembly stresses as a result of different clamp designs, the broad goal of this study was to determine how the different clamp designs affect the high cycle fatigue life of the stem-handlebar assemblies. The key findings were that 1) both stems had similar assembly effects, 2) fatigue lifetimes were similar for both assemblies under constant amplitude loading but the lifetimes differed by 19% under variable amplitude loading, and 3) variable amplitude load fatigue lifetimes were predicted to within about 3% for one stem and to within 33% for the other based on constant amplitude load fatigue test results. Before discussing the importance of these findings, several methodological issues should be critically examined.

TABLE 3—*Cumulative damage and life predictions for both the 1 and 2-bolt stem-handlebar assemblies under variable amplitude loads.*

		Damage ($n_i/N_{f,i}$)	
Max Load, N	Count	1-Bolt Stem	2-Bolt Stem
949	221	1.01E-04	1.21E-04
1402	8	3.30E-05	3.84E-05
1523	8	5.24E-05	6.09E-05
1596	1	8.50E-06	9.84E-06
1840	1	1.88E-05	2.16E-05
	Sum	2.14E-04	2.52E-04
	Lifetime, sequences	4674	3973

TABLE 4—*Summary statistics of sequences to failure and locations of crack initiation relative to the X-axis for variable amplitude load fatigue experiments with both the 1 and 2-bolt stems.*

	1-Bolt Stem		2-Bolt Stem	
	Sequences to Failure	Angle	Sequences to Failure	Angle
Average	4806	168°	5920	152°
Maximum	8132	174°	9511	159°
Minimum	1926	163°	3330	145°
Median	4203	169°	5442	156°
Standard deviation	2333	4.45°	2348	6.84°

Methodological Issues

Because assembly stress depends on the clamping force, the force must be consistent to ensure repeatable assembly stress. Tightening a bolted assembly to a specific torque does not ensure the same tension in the bolt [7,8] so that the assembly stress would be inconsistent. To insure constant assembly stress, bolt force transducers were designed and built to enable repeatable tightening force in the stem clamp bolt(s) that secure the handlebar.

To ensure proper quantification of assembly effects, the proper tightening of the stem bolt(s) had to be determined. Manufacturers recommend a tightening torque of 9.0–11.4 Nm (80–100 in.-lb). To generate the maximum assembly stress and hence the most conservative fatigue life, we used 11.4 Nm for all experimental procedures.

Presumably, the stress concentration would be greatest at the edge of the interface between the stem and the handlebar, and the stresses would vary around the handlebar. To calculate the stress at a point on the outer surface of the handlebar close to the stem in two directions, small rosette strain gages were mounted onto a handlebar. Physical limitations kept the midpoint of the strain gages 1.6 mm away from the edge of the stem. Therefore, the maximum magnitude of the applied stress may have been underestimated.

Although constant amplitude load testing may be useful for product qualification, prediction and testing of fatigue life under variable amplitude loading were of interest because results from constant amplitude load testing may not correctly indicate the relative merits of two different assemblies [6]. To develop a variable amplitude load testing procedure and to predict the fatigue life of the stem-handlebar assembly under variable amplitude loading, it was important to use realistic loading. Downhill ride data recorded from seven different riders in the standing posture were used for this study [4]. Inasmuch as downhill riding is intuitively one of the more damaging types of riding for the stem-handlebar assembly owing to the higher speeds, basing a fatigue life prediction on downhill ride data would be conservative. The seven riders selected for the downhill database were of similar height (average 180 cm) and weight (average 75 kg) and all were experienced riders. The terrain for the trials consisted of a straight trail with an 8% downhill grade containing rocks, ruts, and washouts. Although the downhill ride database did not represent handlebar loads for all riding conditions and all riders, it was nevertheless appropriate for the purposes of this study, where a comparison of the effects of two different stem designs on the variable amplitude load fatigue life was of interest.

To simplify the variable amplitude load fatigue life prediction, stem effects were not explicitly used. However the prediction accounted for the assembly effects implicitly because it was based on fatigue data from the assembled components. A prediction using the quantified assembly effects (i.e., assembly stress and stress concentration) would make the prediction based on stress (rather than load) to account for the different stress ratio and maximum stress in each assembly and at each point. Basing the prediction on

load rather than stress was advantageous because it enabled a more direct comparison to the results from both the constant and variable amplitude load fatigue tests.

To simplify the design of the test fixture, it was loaded only in compression. However, the downhill ride database contained both compressive and tensile loads. To establish a meaningful variable amplitude load fatigue test, the load sequence had to produce a similar amount of damage as the load history in the downhill ride database and also had to represent the variability of the loading. A sequence that satisfied these criteria was established based on rainflow counting, Walker equivalent stress, and range filtering. Alternatively, each set of maximum and minimum stresses could have been truncated at zero (for minimums less than 0), thereby eliminating the need for a tensile load. However, this procedure would have produced less damage than the procedure used because damage due to some of the stress ranges would have been reduced arbitrarily.

Importance/Interpretation of Results

The primary difference in the assembly stresses created by the two stems was in the pattern of the transverse stress (Fig. 5). Transverse stresses resulted from the effects of secondary bending, caused by clamping, which distorted the cross sectional shape from circular (e.g., oval). As a result, the transverse stress was either positive or negative depending on the angular position. The two positive peaks at 120° and 300° for the 2-bolt stem alternating between two negative peaks suggests that the handlebar was deformed into approximately an oval shape by the clamping process. In contrast, the transverse stresses induced by clamping the 1-bolt stem do not exhibit the negative-positive-negative-positive peak behavior, suggesting that the deformed cross section of the handlebar was not oval. These differences in the distortion of the cross section are not surprising considering that the 2-bolt clamp was symmetrical whereas the 1-bolt clamp was not (Fig. 1).

The close comparison of the stress concentration effects (Fig. 6) was surprising considering the differences in both the clamp design and the radii at the edge of the clamps. As mentioned earlier, the edge of the clamp portion of the 1-bolt stem was a sharp corner whereas the edge of the 2-bolt stem had a radius of about 1 mm. Because of the sharp corner, it was expected that the stress concentration would be higher for the 1-bolt stem. Two possible reasons may explain why this expectation was not realized. One is that the stress concentration for the corner was greater but this was not detected because the gages did not measure strain at the edge of the stem as mentioned earlier. The other is that the stress concentrations in fact were the same, perhaps because the thicker clamp of the 2-bolt stem was stiffer than the thinner clamp of the 1-bolt stem. The latter of these explanations is more likely because if there was a higher stress concentration for the 1-bolt stem, then this stem would have exhibited a shorter fatigue life in the constant amplitude load tests. Because both the 1-bolt and 2-bolt stems had comparable fatigue lifetimes (Fig. 8), an unmeasured higher stress concentration for the 1-bolt stem is unlikely.

Notwithstanding the differences in the design between the two stems, the high cycle fatigue lives in the constant amplitude load tests were remarkably similar (Fig. 7). The similarity in the life can be traced to the close comparison in the equivalent stresses (Fig. 10). Although the median locations of crack initiation did not correspond exactly to the locations of the peak values in the equivalent stresses, the equivalent stress curves both were characterized by a plateau region in the vicinity of the peak value that extended from about 160–180° for the 1-bolt stem and from about 150–170° for the 2-bolt stem. Thus the cracks initiated in the region of the peaks if not exactly at the peaks. The data in Fig. 7 suggest that the high cycle fatigue life for a particular handlebar is independent of the stem. If this result can be generalized, then it would be very useful to product qualification in the bicycle industry because manufacturers could test a particular handlebar with an arbitrary stem rather than for the range of stems actually used. Before the present results can be generalized, however, additional testing is warranted. This additional testing would require a wider range of stems for a particular handlebar and also would include different handlebars.

Not only were the high cycle fatigue results similar for the average life, but also the results were similar for the variability in life. As a result of differences in material composition, surface effects, and other factors, fatigue life even under carefully controlled loading inherently has variability, and the variability usually increases as lifetimes become longer [7,14]. The standard deviations were 8664 cycles and 7293 cycles for the 1-bolt and 2-bolt stems, respectively, for the shortest lifetimes and 387211 cycles and 207421 cycles for the 1-bolt and 2-bolt stems, respectively, for the longest lifetimes from constant amplitude load testing. For variable amplitude load testing the standard deviation was 2348 sequences for the 1-bolt stem and 2333 sequences for the 2-bolt stem. The close comparison in the standard deviation suggests that the reliability of the two stem-handlebar assemblies would be similar.

The stem clamp assembly effects likely reduced the constant amplitude load fatigue strength substantially. Comparing the large difference in equivalent stress that occurs when the effects from either stem are included in the stress computation to when they are ignored (Fig. 10), suggests that the stem effects have a significant effect on fatigue strength. An early experimental study of clamped collars onto steel shafts loaded in rotating bending demonstrated that the fatigue strength was reduced to 55% of the fatigue strength without the clamped collar for a life of 10^7 cycles [15]. Therefore, the large effect of assembly on fatigue strength as suggested by the large difference in equivalent stress with and without the stem is not without precedent. At the very least, a design engineer must use a fatigue strength that is substantially reduced from what occurs in the absence of assembly and the specific reduction used in design may depend on the specific stem employed. Design variables such as the radius of the clamp edge, structural stiffness of the clamp, and angular position of the clamp bolt could all influence the assembly stress effect and hence the fatigue behavior.

The results for the variable amplitude load fatigue tests also demonstrated that the average fatigue lives for the two stem assemblies were comparable, differing by only 19%, but that the 2-bolt stem assembly had the longer life. This result is in contrast to that from the constant amplitude load fatigue tests where the mean lives were longer for the 1-bolt stem-handlebar assembly than those of the 2-bolt stem-handlebar assembly. It is generally recognized that variable amplitude load testing can lead to differences in ranking when compared to constant amplitude load testing [6], as was the case in the present study. However, the shift in the present study was relatively minor compared to shifts that have been documented in other tests. For example, cast aluminum test coupons tested in 3-point bending tested in three states (not welded, transverse butt welded, and repair welded) all demonstrated comparable fatigue lifetimes under constant amplitude load tests but under variable amplitude load tests, the fatigue lifetimes of both the not welded and repair welded coupons exceeded that of the transverse butt welded coupons by a factor of 3 [6].

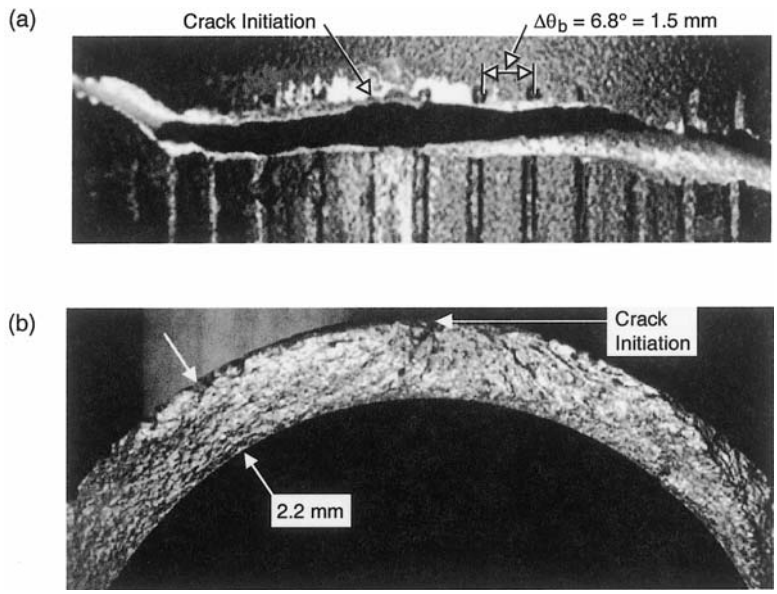

FIG. 11—*a) Outer surface of a handlebar failed in constant amplitude load fatigue, and b) fracture surface of the handlebar shown in (a).*

The comparison between the measured lifetimes for the constant and variable amplitude load tests has relevance to the test method used to qualify stem-handlebar assemblies by the bicycle industry. To qualify the stem-handlebar assembly for use in the field, some type of mechanical testing must be conducted, the simplest of which is constant amplitude load testing. Constant amplitude load testing is attractive because the simplicity lends itself to a relatively low test cost. As a result of the low cost, a constant amplitude load testing system is affordable to most companies, thereby providing the capability of in-house qualification of designs. However, this method of testing can be justified only if it provides an appropriate ranking of products with similar failure locations as those that occur under variable amplitude load testing [6]. Although the ranking of the two stems shifted between the constant (Fig. 7) and variable amplitude load tests (Table 4), nevertheless the shift in the ranking was relatively minor as noted above. Consequently, the additional complexity of variable amplitude load fatigue tests does not seem warranted for this application.

Failure analysis from both types of tests indicated that cracks initiated in nearly the same locations for both stem designs with the most common angular location differing by only 6°. The most common location for fatigue crack initiation was at the end of the grooves in the handlebar for both stems for both types of tests (Fig. 11). This was expected for the 1-bolt stem, where the edge of the clamp coincided with the end of the grooves, but it was surprising for the 2-bolt stem where the clamp overlapped the grooves by 7.5 mm. The grooves induced a stress concentration particularly at their ends, which acted like a notch tip. This elevated the nominal stress resulting in the end of the groove being especially prone to failure. The use of a handlebar without grooves should result in circumferential failure locations that match those measured herein because the grooves were closely spaced and present around the circumference so that the angular location of crack initiation was not highly biased (Fig. 11). Because the constant amplitude load tests produced failure locations similar to those of the variable amplitude load tests, their use as a meaningful test for qualifying stem-handlebar assemblies is justified further.

As a final argument to justify the use of constant amplitude load tests, the variable amplitude load fatigue lifetimes were predicted based on the load-lifetime data collected in the constant amplitude load tests and compared to the experimentally measured lifetimes. Inasmuch as the predicted lifetimes were comparable to those measured, differing by only 33%, this result further justifies the use of constant amplitude loading in product qualification. Moreover, both life predictions were conservative in that predicted life was less than measured life. Therefore, the methodology used to make these predictions could serve well in the design process.

Caution must be exercised in interpreting the variable amplitude load fatigue lifetimes measured based on the downhill ride database. This is because this database represents only one of several loading conditions commonly encountered in off-road cycling. Other common loading conditions include uphill climbing in either the seated or standing position at relatively low speed, and cruising over relatively flat and smooth terrain. Clearly, these loading conditions would be expected to develop lower dynamic loading than the high-speed downhill riding used to develop the database for the fatigue life predictions herein. Accordingly, to obtain a realistic prediction of the expected service life of these assemblies, the loading for each riding condition would need to be determined together with the time spent in each riding condition. These additional data could be used advantageously to determine time to failure under representative use.

Acknowledgment

We are grateful to Answer Products and in particular Scott Boyer and Rick Pedigo for the financial support of this project. We also thank Mark LaPlante of the Cannondale Corporation for supplying the handlebars.

References

[1] "Specialized Announces Bike Brake, Handlebar Recall," U.S. Consumer Product Safety Commission, Office of Information and Public Affairs, Release # 95–155, 1995.

[2] "Trek Bicycle Corp. Announces Recall of Road Bikes and Handlebar Stems," U.S. Consumer Product Safety Commission, Office of Information and Public Affairs, Release # 00–192, 2000.
[3] ISO-4210: Safety Requirements for Bicycles, International Organization for Standardization, Geneva, Switzerland, 1996.
[4] De Lorenzo, D. S. and Hull, M. L., "Quantification of Structural Loading During Off-Road Cycling," *Journal of Biomechanical Engineering*, Vol. 121, No. 4, 1999, pp. 399–404.
[5] Petrone, N., Tessari, A., and Tovo, R., "Acquisition and Analysis of Service Load Histories in Mountain-Bikes," *Proceedings of the XXVth AIAS National Conference—International Conference on Material Engineering,*Vol. II, Galatina, LE-Italy, 1996, pp. 851–858.
[6] Shütz, D. and Heuler, P., "The Significance of Variable Amplitude Fatigue Testing," *Automation in Fatigue and Fracture: Testing and Analysis, STP 1231*, C. Amzallags, Ed., ASTM International, West Conshohocken, PA, 1994, pp. 201–220.
[7] Almen, J. O. and Black, P. H., *Residual Stress and Fatigue in Metals*, McGraw-Hill, New York, NY, 1963.
[8] Grover, H. J., *Fatigue of Aircraft Structures*, U.S. Government Printing Office, Washington, D.C., 1966.
[9] Sines, G. and Waisman, J. L., *Metal Fatigue*, McGraw-Hill, New York, NY, 1959.
[10] *Metallic Materials and Elements for Aerospace Vehicle Structures (Mil-HDBK-5F)*, U.S. Department of Defense, MIL-HDBK-5 Coordination Activity, Wright-Patterson AFB, OH, 1990.
[11] Heuler, P. and Seeger, T., "A Criterion for Omission of Variable Amplitude Loading Histories," *International Journal of Fatigue*, Vol. 8**,** No. 4**,** 1986**,** pp. 225–230.
[12] Palmgren, A., "Die Lebensdauer von Kugellagern," *Zeitschrift des Vereins Deutscher Ingenieure*, Vol. 68**,** No. 14**,** 1924**,** pp. 339–341.
[13] Miner, M. A., "Cumulative Damage in Fatigue," *Journal of Applied Mechanics*, Vol. 67**,** 1945**,** pp. A159.
[14] Dowling, N. E., *Mechanical Behavior of Materials*, 2nd Edition, Prentice-Hall, Upper Saddle River, New Jersey, 1998.
[15] Lea, F. C., "The Effect of Discontinuities and Surface Conditions on Failure Under Repeated Stress," *Engineering*, Vol. 144**,** No. 2**,** 1937**,** pp. 87–90, 140–144.